



Molecular, Histopathological, and Immunohistochemical Characteristics of Fowl Adenovirus, Serotype 7 (Species E), in Egyptian Broiler Breeders: First Report

Mohamed Helmy¹, Amany Adel², Azza Hassan^{3*} and Rawhiya Doghim³

¹VACSERA The Holding Company for Biological Products and Vaccines, Giza, Egypt.

²Reference Laboratory for Veterinary Quality Control on Poultry Production, Animal Health Research Institute, Agriculture Research Center, Giza 12618, Egypt.

³Pathology Department, Faculty of Veterinary Medicine, Cairo University, Giza, 12211, Egypt.

Abstract

FOWL adenoviruses recently became a hot topic for most Egyptian researchers and investigators, where the Egyptian poultry industry suffered from several outbreaks of fowl adenovirus (FAV) attacks in commercial broiler flocks. As vertical transmission from the parent flock represents the most common infection, the present study aimed to investigate the molecular characterization of FAV species isolated from commercial broiler breeder flocks in northern Egypt from 2021 to 2023. Organ samples and swabs from 10 breeder flocks have been examined in real-time. Quantitative reverse transcription polymerase chain reaction (RT-qPCR) revealed positivity for fowl adenovirus, with variable PCR cycle threshold (CT) values ranging from 10 to 36. The loop1 (L1 regions) on the hexon gene of the ten positive samples have been amplified by conventional PCR, which resulted in only three positive samples at molecular size 800 bp, and only one representative PCR product has been sequenced for the L1 region. The genetic characterization revealed the first record for the existence of serotype 7 of FAV-species E in Egypt. The sequenced sample is similar to strain 12-10101 with an identity of 97%. Histopathological examination revealed inclusion body hepatitis associated with abundant apoptosis, hydropericardium, myocarditis, pancreatic acinar cell necrosis, glomerulonephritis, and acute tubular necrosis. FAV antigen was demonstrated in examined tissues using avidin-biotin-peroxidase. In addition, cleaved caspase-3 immunohistochemical staining revealed strong positive immune reactivity in the liver, pancreas, and kidneys. Proliferating cell nuclear antigen (PCNA) immune staining revealed positive immune reactivity in the regenerating renal tubules.

Keywords: Fowl Adenovirus, Histopathology, Caspase-3, PCNA. Immunohistochemistry.

Introduction

Fowl adenoviruses (FAdV) are common infectious agents in poultry. Although fowl adenoviruses can normally be isolated from healthy avian hosts, they also act as primary pathogens in a variety of avian species, including chicken, quail, and turkey. In chickens, avian adenoviruses are the causative agents of two diseases: inclusion body hepatitis (IBH) and hydropericardium syndrome (HP).

Adenovirus is a double-stranded DNA, non-enveloped, icosahedral virion with a diameter ranging from 70 to 90 nm and 252 capsomeres with a

special arrangement [1]. The main structural proteins are hexon (II) and fibre (I), with a penton base (III) linked by non-covalent bonds, and minor proteins IX, IVa2, VI, IIIa, and VIII [2].

Members of the Adenoviridae family are classified into five genera based on their genome sequence: siadenovirus, Mastadenovirus, Aviadenovirus, Atadenovirus, and ichtadenovirus [3,4]. The genus Avianadenovirus is classified serologically into 12 serotypes, including 1–7, 8a, 8b, and 9–11, clustered into five groups (A–E) on a molecular basis [5]. All serotypes have a direct relationship with inclusion body hepatitis (IBH)

*Corresponding author: Azza Hassan, E-mail: azzahassa1999@gmail.com, Tel.: 01100782840

(Received 28/04/2024, accepted 04/07/2024)

DOI: 10.21608/EJVS.2024.285912.2044

©National Information and Documentation Center (NIDOC)

outbreaks [6]. FAdV can be transmitted vertically or horizontally [7]. Cross-protection between different serotypes has a narrow range [8].

Chicken breeds can affect the mortality and severity of FAdV infections [7]. The most well-known broiler breeds in Egypt are Indian River, Cobb, Hubbard, Arbour Acres, and Ross from the most international breeders' companies [9].

Fowl adenoviruses have been recorded all over the world [1]. In Egypt, there have been many records for different serotypes of FAdVs. The dominant serotypes 2 and 11 of species D have been recorded in commercial broilers in most studies in Egypt [10, 11, 12, 13].

Serotype 8a of species E was isolated from a broiler flock [14], and it was recorded in other broiler flocks during 2019–2020 [13]. The most important pathogenic serotype 4 has been recorded as a sole case in a broiler flock in Egypt in 2021 [15]. The other serotypes, including 1, 3, and 8b, have been detected in different broilers, breeders, and layer flocks as a result of passive surveillance accomplished in all the governorates of Egypt during 2019–2020 [13].

The current study aims to investigate the molecular, histopathological, and immunohistochemical characteristics of the fowl adenovirus, Serotype 7-Species E Strain, in broiler breeder flocks (Avian 48 and Indian River) breeds in Egypt.

Material and Methods

Sampling and epidemiological data

During 2021 - 2023, several FAV outbreaks were reported in broiler and broiler breeder flocks in Egypt. Ten commercial broiler breeder flocks, of different ages and localities (Behera, Menofia, Alexandria and Marsmatroh), were submitted for investigations. These flocks revealed a sudden onset of mortalities exceeding the normal mortality percentage related to the breeder's standard catalogues. The detailed data of these broiler breeder flocks, including location, flock age, breeds, stocking, and number of samples, is illustrated in (Table 1). Fifty freshly dead birds were examined, and post-mortem lesions were recorded. Tissue samples from the heart, liver, kidney, and pancreas were obtained and divided into two parts. The first part was kept on ice and transported to the Reference Laboratory for Veterinary Quality Control of Poultry Production, Dokki-Giza (R.L.Q.P.) for molecular characterization of FAdV, the second part was preserved in a 10% neutral buffered formalin solution for histopathological examination.

Ethical approval

All samples were collected under the permission of the local license from the Institute Animal Care

and Use Committee (IACUC). Faculty of Veterinary Medicine, Cairo University, Egypt

Vet CU 25122023809.

Molecular detection and analysis of fowl adenovirus

Extraction of viral nucleic acid

The viral nucleic acid was extracted using the QIAamp mini elute spin kit (Qiagen, GmnH, Germany, Cat. No. 57704), following the manufacturer's instructions: 200 μ l of the swab sample fluid or tissue homogenate supernatant were incubated with 200 μ l of AL lysis buffer and 25 μ l of Qiagen protease at 56 oC for 15 min. Then, 250 μ l of absolute ethanol was added to the lysate. The mixture was then washed and centrifuged. Nucleic acid was finally eluted with 100 μ l of elution buffer.

Real-time qPCR for detection of fowl adenovirus

The extracted nucleic acid in ten suspected samples was examined by real-time qPCR for detection of fowl adenoviruses, following the instructions of KylvFAdv, Art .No.31744.

Amplification of nucleic acid using conventional PCR

Conventional polymerase chain reactions (PCR) were performed using specific primers for the L1 region of the hexon gene of fowl adenoviruses [13]. The nucleotide sequences of these primers are adeno-F- 5'-ACATGGGAGCGACCTACTTCGACA-3' and adeno-R- 5'-TCGGCGAGCATGTACTGGTAAC-3'. PCR was accomplished by EmeraldAmp Max PCR Master Mix (Takara, Japan) using the following conditions: A 25- μ l total volume of PCR reaction included 12.5 μ l of EmeraldAmp Max PCR Master Mix, 1 μ l of forward and reverse primers (in working concentration 20 pmol), 6.5 μ l of PCR grade water, and finally added 3 μ l of extracted DNA. The reactions were run in the Biometra T3000 thermal cycler in these steps: denaturation step at 95 OC for 5 min, then 35 cycles were run as follows: Secondary denaturation at 94 OC for 30 sec., annealing at 60 OC for 45 sec., and extension at 72 OC for 1 min., then a final extension step at 72 OC for 10 min.

Sequencing of the Loop1 region of hexon gene

The amplified PCR products with the appropriate size were subsequently purified using a QIAquick Gel Extraction Kit (QIAGEN, Hilden, Germany, Cat. No./ID: 28704). The purified PCR products were subjected to sequencing reactions using a Big Dye Terminator v3.1 Cycle Sequencing Kit (Applied Biosystems, Foster City, CA, Cat. No. 4337455). According to the manufacturer, the reaction product was purified by exclusion chromatography in the DyeEX 2.0 Spin Kit (50) (Cat. No.: 63204). The recovered materials were sequenced using a 3500 XL DNA Analyzer (Applied Biosystems).

Sequence analysis and Phylogeny of the Loop1 of hexon gene

BioEdit version 7.0 [16] was used for multiple sequence alignment by the ClustalW method and percent identity matrices between different viruses. Neighbour-joining Phylogenetic trees were constructed using the distance-based method in MEGA version 11 [17], with a bootstrap of 1000 replicates. The trees included the sequenced samples from this study plus the sequences of strains for the serotypes of adenoviruses downloaded from Genbank (NCBI).

Histopathological examination

Tissue specimens from the liver, heart, pancreas, and kidneys were fixed into a 10% neutral buffered formalin solution and kept at room temperature for 24–48 hours. Specimens were subjected to the traditional paraffin-embedded technique for tissue processing. Samples were dehydrated in ascending concentrations of ethanol, cleared in xylene, sectioned to 4 µm thickness, and slide sections stained by hematoxylin and eosin (H&E) examined under light microscopy [18].

Immunohistochemical analysis

Preparation of the hyperimmune serum

FAV hyper-immune serum was prepared in two female New Zealand white rabbits weighing 3.5–4 kg [20] using the FAV whole virus inactivated vaccine under the commercial name Dolguban-H oil inactivated vaccine (KBNP, INC., Korea). The experimental procedures were carried out in the experimental animal house of the Central Laboratory for Evaluation of Veterinary Biology (CLEVB), Abbasia, Egypt. A control blood sample of 5 ml was obtained first, followed by immunization schedules. After the vaccine reaches room temperature, under the umbrella of tranquillizer accompanied by local anaesthesia of the injection site, the schedule is followed by subcutaneous injection of 0.5 ml/dose in the first week, up-dose titration to 1 ml/dose after 14 days from the first immunization, and then 1.5 ml/dose in the fourth and fifth weeks of the experiment. Ten days later, a blood sample of 10 ml was aseptically collected from the marginal ear vein under sedation in a tube, after blood clot formation by centrifugation at 2700 rpm, and then kept in the refrigerator [20]. Serum antibody titer was tested by FAdV ELISA CK 132, manufactured by Biocheck (UK), serial number FS8226, manufactured date: May 11, 2021, expiry date: May 5, 2022, and procedures were followed according to the instructions of the manufacturer [21]. After the detection of a high level of antibody titer, rabbits were humanely euthanized, and hyperimmune serum was collected and used in avidin-biotin

immunohistochemical staining for the detection of the viral antigen in the tissues [20,21].

Immunohistochemical examination

Immunohistochemical staining for the demonstration of fowl Adenovirus particles, caspase-3 activity (an apoptotic marker), and PCNA (a proliferation marker) was carried out as described by [22,23]. Briefly, the paraffin-embedded tissues were sectioned on positively charged glass slides at a size of 4 microns, deparafinized, and rehydrated with graded concentrations of alcohol. After that, the sections were blocked by using a 3% hydrogen peroxide solution (H₂O₂). The sections were then incubated with anti-fowl Adeno antibody (dilution 1:200), anti-caspase-3 antibody (Enzo Life Science, Cat. No. ADI-APP-113, RRID: AB_10615972, USA), and mouse monoclonal anti-PCNA antibody (ABIN214368, antibodies-online, USA). The immune reaction was visualized using diaminobenzidine (DAB).

Results and discussion

Molecular analysis of the fowl adeno virus

Real-time qPCR

The suspected ten samples examined by real-time qPCR showed positive results with various Ct values, as shown in Table (2).

Conventional PCR

The positive samples were amplified by conventional PCR for the L1 region of the hexon gene, and the results showed positive for only three samples that had the earlier ct values in real-time qPCR.

Sequence of Loop1-region of Hexon gene

The phylogenetic tree of the nucleotide sequence illustrated in (Fig. 1) revealed that the detected virus was genetically related to FAdV-species E and definitely more related to serotype 7.

Sequence analysis of Loop1-region of Hexon gene

Comparing our target virus with other viruses related to the different species of FAdV, we found that our target virus was highly similar to the strain 12-10101 of FAdV, species E, with an identity of 97%. Additionally, it was highly similar to strains of serotype 7 that underlay FAdV-species E, with identity = 93–95%, as shown in (Fig.2). However, the similarity with other circulating Egyptian viruses was reduced, as the nucleotide sequence identity was 83.5%, 78%, 64.9%, 53.5%, 58.5%, and 62.6% for FAdV species 8b/E, 8a/E, D, C, A, and B, respectively, as shown in (Fig.3). Even the amino acid sequence alignment of the L1 region in (Fig.3) showed that our target virus possessed the most conservative areas with the strains of serotypes 7 and 8b.

Histopathology

Various histopathological alterations were demonstrated in different organs, particularly the liver, heart, pancreas and kidneys. The liver showed extensive thickening of the Glisson's capsule with faint pink fibrinous exudate mixed with intense inflammatory cell infiltration, mostly heterophils and lymphocytes (Fig.4a). Various histopathological lesions ranging from diffuse vacuolar degeneration of hepatocytes to massive bridging hepatocellular necrosis associated with intense leucocytic cellular infiltrates were demonstrated (Figs.4b and 4c). Hepatocellular necrosis was frequently demonstrated in the centrilobular area with fragmentation and dissociation of the necrotic hepatocytes, in addition to the presence of numerous apoptotic cells (Fig.4d). One of the most frequently demonstrated lesions was inclusion body hepatitis, with the presence of numerous large basophilic intranuclear inclusions (Figs.4e and 4f). Inclusion body hepatitis is concurrently associated with abundant apoptosis (Fig. 4g).

The heart revealed hydropericardium with marked thickening of the visceral epicardium by edematous fluid associated with scattered lymphocytic cell infiltration (Fig.5a). Various alterations were demonstrated in the myocardium, ranging from interstitial edema (Fig. 5b) to vacuolar degeneration of cardiomyocytes associated with numerous apoptosis (Fig. 5c). Interstitial myocarditis with intense infiltration of cardiomyocytes with heterophiles and lymphocytes was a common finding (Fig.5d).

Similar histopathological alterations were also demonstrated in the pancreas, which revealed congestion of blood vessels associated with interstitial edema and disruption of pancreatic acinar cells (Fig.5e). Multifocal areas of pancreatic necrosis with complete loss of cellular architecture that appeared intensely eosinophilic with nuclear pyknosis were frequently demonstrated (Fig.5f). In some sections, the focal pancreatic necrosis was intensely infiltrated with macrophages and lymphocytes (Fig. 5g). Abundant apoptosis of pancreatic acinar cells was frequently demonstrated (Fig. 5h).

The kidneys showed outstanding histopathological alterations that were demonstrated in the renal glomeruli and tubules. Proliferative and membranoproliferative glomerulonephritis, with markedly swollen glomeruli and pronounced mesangial cell proliferation as well as obliteration of the Bowman's spaces, were characteristically demonstrated (Figs. 6a and 6b). In addition, extensive degenerative and necrotic changes were demonstrated in the renal tubules. These alterations varied from extensive vacuolar degeneration to extensive necrosis of the renal tubular epithelium

(Figs. 6c and 6d). The necrotic renal tubules were intensely infiltrated with inflammatory cells (Fig. 6e). The necrotic renal tubules, alternating with the regenerative renal tubules, which are lined by large, basophilic vesicular nuclei, were also demonstrated (Fig. 6f).

Immunohistochemistry

Immunohistochemical detection of adenovirus in the tissues

Immunohistochemical examination revealed the presence of adenoviral antigens in different organs, particularly the liver, heart, pancreas, and kidneys. Extensive intranuclear and cytoplasmic staining was demonstrated in the infected hepatocytes, vascular endothelial cells, and intravascular leukocytes (Fig. 7a). Additionally, intense brown intranuclear adenoviral antigen was demonstrated in the cardiomyocytes, endothelial cells, and infiltrating inflammatory leukocytes (Figs. 7b and 7c). A strong brown intranuclear adenoviral antigen was also demonstrated in the pancreatic acinar cells (Fig. 7d) and the infiltrating leukocytes (Fig. 7e). The kidneys, revealed brown intranuclear and cytoplasmic adenoviral antigen in the glomerular capillary endothelium (Fig. 7f) and renal tubular epithelium (Fig. 7g).

Immunohistochemical expression of cleaved caspase-3 and PCNA

Increased caspase-3 expression, with strong brown nuclear and cytoplasmic staining, was demonstrated in the hepatocytes (Fig. 8a) and pancreatic acinar cells (Fig. 8b). Interestingly, the more numerous caspase-3-positive cells, with intense brown staining, were demonstrated in the area of acute hepatitis and pancreatitis (Fig. 8c). Similarly, abundant caspase-3-positive cells were demonstrated in the lumen of renal tubules (Fig. 8d). On the other hand, PCNA-positive cells with strong brown nuclear staining were demonstrated in the regenerating renal tubules (Fig. 8e).

Discussion

The suspected samples under this study have been examined by real-time qPCR as a rapid, sensitive molecular technique for confirmation of the fowl adenovirus infection [24]. It revealed 100% positivity in our examined samples with different CT values, which depended on the viral load in each sample. Consequently, all the positive samples have been amplified by conventional PCR for the L1 region on the hexon gene of the Fowl adenovirus for further genetic sequencing and analysis. However, only three positive samples have been amplified as they contained the highest viral load, which is required for successful amplification due to the large molecular size as in our study [25]. The L1 region was our target for molecular characterization because it is the most variable area on the hexon gene and has

a strong impact on the genetic and antigenic classification of fowl adenoviruses [26].

Different avian adenovirus species have been extensively detected in Egypt during the last few years [10,14,12,13]and[15]. Since its detection, FAdV-species D has been the most commonly distributed type in Egypt [13]. Serotype 8a of species E was detected in Egypt for the first time in 2018[14], and then different serotypes 8b, 3, and 1 of species E, B, and A, respectively, have been recorded through passive surveillance along with Egypt during 2019–2020, based on examination of 340 suspected samples [13].

In this study, the detected virus was genetically related to FAdV-species E, closely related to the Egyptian serotype 8b strains, and strongly similar to the serotype 7 in worldwide strains, as shown in the similarity table in Figure 2. Interestingly, it was found that the target virus in this study was genetically related to the recombinant strain 12-10101 (accession no.MK572860), with the highest identity percentage of 97%. This strain was recorded in Germany in 2019 and classified as serotype 7 of FAdV-species E with recombination evidence between species E and [27].

Avianadenoviruses were classified based on their molecular structure into 5 species, which were further divided according to the cross-neutralisation test into 12 serotypes: fowl adenovirus A (FAdV-1), fowl adenovirus C (FAdV-4 and -10), fowl adenovirus B (FAdV-5), fowl adenovirus D (FAdV-2, -3, -9, and -11), and fowl adenovirus E (FAdV-6, -7, -8a, and -8b) [28]. Each of the 12 FAdV serotypes has been recorded to be related to inclusion body hepatitis (IBH) outbreaks [6]. Group D and E species were involved in hepatitis-hydropericardium syndrome (HHS) and hydropericardium syndrome (HPS) in the intensified poultry region [29]. Some serotypes had been considered highly pathogenic, including FAdV-4, -2, -7, and -11 [30]. Regarding serotype 7, there are few reports globally [31]. More recently, [32] reported that fowl adenovirus E (FAdV-8a) is associated with gizzard erosion. Unfortunately, up to date, there has been no unanimously identified virulence factor identified by researchers that allows FAdVs to be a "black box"[33]. FAdV-7 and FAdV-8A are closely related and constitute a cluster of adenoviruses from species E [34]. In Egypt, the dominant FAdv species were species D and species 8a and 8e, with recently detected serotypes 1, 3, and 8b [13].

Regarding the histopathological alterations demonstrated in the current study, the liver revealed thickening of the Glissons capsule, which is in agreement with [35]. This thickening could be attributed to the exaggerated inflammatory response of acute fibrinohemorrhagic hepatitis induced by

viral replication in hepatocytes, as explained by [36,37,38].

Massive bridging hepatocellular necroses associated with numerous apoptosis are also characteristic findings in the present study. These alterations are attributed to the viral tropism in hepatocytes and its cytolytic nature. Moreover, FAV can induce autophagy and apoptosis with severe inflammation, resulting in massive necrosis. Apoptosis induced by hypervirulent FAVs is mainly due to the major role of Fowl Adeno Protein X (FAdV PX), which represents one of 11 structural viral proteins (hexon, fibre 1, fibre 2, pIIIa, IVa2, pTP, pVI, pVII, pVIII, pX, and penton base) of the Adenovirus [30]. PX protein is almost localised in the nucleus of virus-infected cells. PX nuclear translocation is a crucial step for apoptosis induction throughout activation of the caspase-3 pathway which represents an important step for completing the viral replication cycle [39]. Despite the previous mechanism, the definite mechanism underlying the induction of apoptosis is still elusive [40]. The inflammatory mediators, including both interleukin 1 beta (IL1B) and macrophage inflammatory protein-2 (MIP-2), are produced from many inflammatory cells, such as monocytes, epithelial cells, and even hepatocytes and endothelial cells, during the response to fowl adenovirus infection, as previously reported by [37,38].

The presence of large basophilic intra-nuclear inclusions within infected hepatocytes in the present study is in accordance with [41,42]. These inclusions are due to viral replication within the hepatocyte nucleus, which is confirmed in the immunohistochemically – stained sections. The variation in size and number of these inclusions mainly depends on the hepatocyte production intensity of the inclusion [43]. Moreover, [44] fully described the intranuclear inclusion as a round and compact "bird eye" that occupied nearly the entire nucleus.

Regarding the pathological findings in the heart, which include hydropericardium with thickening of the visceral pericardium associated with lymphocytic cell infiltration, they are in accordance with [45]. The pericardial effusion is mainly due to an increase in the permeability of the vascular endothelial cells, which results in plasma exudation [46]. Furthermore, the disturbance in albumin due to FAV infection decreases colloidal osmotic pressure, which may have a supplementary role [47].

Myocardial edema with vacuolar degeneration of cardiomyocytes and interstitial myocarditis demonstrated in the present study are in coincidence with [48,49]. Despite the lower susceptibility of cardiomyocytes (CM) to fowl Adenovirus FAdV [46], once virus proliferation occurred, it resulted in increased mRNA expression of many inflammatory

cytokine genes (interleukin-1B, interleukin-6, interleukin-8, and tumour necrosis factor) (*IL1B*, *IL6*, *IL8*, and *TNF*, respectively) and elevation of the myocardial enzymes [50]. IL-1 β induces endothelial cell tissue factors (ECsTF), which results in an increment of vascular permeability [51]. The immunohistochemical results of the present study confirm the viral replication within the cardiomyocytes, the vascular endothelial cells, and the infiltrating mononuclear cells.

Pathological findings in the kidneys in the present study include, proliferative and membrano-proliferative glomerulonephritis were the most prominent alterations in the renal glomeruli, which are in accordance with the findings of [52,41]. Membranoproliferative glomerulonephritis is attributed to hypersensitivity type III, with deposition of the immune complex in the glomerular capillaries after virus initiation of inflammation [19]. This may clarify the hypercellularity of the renal corpuscle, considering its response to FAV virus infection. Moreover, the presence of the adenoviral antigen within the glomerular tuft is confirmed immunohistochemically in the current study.

Alterations in the renal tubules presented in our work varied from vacuolar degeneration to extensive necrosis of the tubular epithelium with intense inflammatory cell infiltration. In accordance with [44,53,54], this could be attributed to the capability of the virus to replicate within tubular epithelial cells of the kidney during virus pathogenesis [55,56,41], and these alterations are confirmed in the immunohistochemically-stained sections. In addition, the virus provokes acute renal damage, which further results in an increase in vascular permeability and inflammatory cell recruitment, as well as the deposition of exudates in the kidney parenchyma [44]. Hyperplastic proliferation of the adjacent renal tubules seems to be a compensatory mechanism.

Being a target organ for the virus due to its faster replication [57], the pancreas is highly vulnerable to adenovirus infection. Pancreatic necrosis and pancreatic edema with subsequent disruption of the pancreatic architecture demonstrated in the present study are following the findings of [14, 41]. Mononuclear cell infiltration appears to be mainly due to an inflammatory reaction caused by FAD, as mentioned by [57,7].

Immunohistochemical results of the current study revealed positive immune reactivity, with intense brown nuclear and cytoplasmic staining. The immune reaction was demonstrated in different organs, particularly the liver, heart, kidneys and pancreas, confirming the presence of FAV-7 virus particles in these organs. These results are in accordance with the findings of [58,59]. Previous studies also confirmed the intracytoplasmic virus particles of FAV-4 [60, 61].

The high expression of PCNA in kidneys demonstrated in our investigation reflected the high proliferation within renal tissue [62]. PCNA represents an essential protein cluster within the nuclei and is mainly incorporated in DNA replication and cell proliferation [63]. PCNA-positive cells demonstrated in renal tubular epithelial cells indicate DNA replication and damage repair of nuclear contents [64]. This regenerative activity occurred in response to the severe tissue damage in the kidney induced by the FAV-7 virus field infection.

Conclusions

FAV-7 related to group E Adeno viruses was prevalent in broiler breeder flocks in this study, associated with massive hepatorenal pathological alterations, hydropericardium syndrome, and severe pancreatitis. Increased mortality rates in young breeders regarding the breeder's standard catalogue, decreased flock performance, and a decline in egg production were the most noticeable observations in producer breeders in Egypt the present study is considered to be the first pathomolecular study on FAV-7 in Egyptian breeders. Further studies are needed to assess the potentiality of FAV serotype prevalence in breeder's farms and grandparent flocks.

Conflicts of interest

No conflicts of interest are disclosed by the authors.

Funding statement

The authors declare that they did not receive any grants, funding, or other forms of assistance in order to prepare this manuscript.

Acknowledgement: For all colleagues in the department.

TABLE1. Epidemiological data of the investigated broiler breeder flocks with relation to (number of birds, flock age, breeds, localities/governorates, season at time of sampling and related necropsy finding in corresponding to mortality percentage

Flock	Age	Breed	Number	Samples number	Location	Season	Mortality	Gross lesion	Initial diagnosis	Egg production
1	37 W	AVIA N 48	10 k	4	Behera	Summer	2% (N: 0.2%)	HP/IBH/As	Real timeqPCR Real timeqPCR	20 % loss
2	10 D	AVIA N 48	10 k	5	Alexandria	Winter	3% (N:0.9)	HP/IBH	Real timeqPCR Real timeqPCR	Breeding
3	38 w	AVIA N 48	15 k	4	Behera	Spring	1.5% (N: 0.2%)	HP/IBH/As	Real timeqPCR	10 % loss
4	13 D	AVIA N 48	5 k	3	Behera	Spring	1% (N:0.9)	HP/IBH	Real timeqPCR Real timeqPCR	Breeding
5	38 w	IR	10 k	10	Marsamatroh	Autumn	3% (N: 0.2%) 1%	HP/IBH/As	Real timeqPCR Real timeqPCR Real timeqPCR	20 % loss
6	32 w	AVIA N 48	8 k	5	Menofia	Winter	(N: 0.2%) 3%	HP/IBH/As		5 % loss
7	2w	IR	7 k	10	Marsamatroh	Winter	(N:0.9) 2%	HP/IBH		Breeding
8	2w	AVIA N 48	10 k	5	Behera	Winter	(N:0.9) 1%	HP/IBH		Breeding
9	32 w	AVIA N 48	10 k	4	Behera	Spring	(N: 0.2%) 3%	HP/IBH/As		10 % loss
10	35 w	IR	15 k	9	Marsamatroh	Spring	(N: 0.2%) 2%	HP/IBH/As		10 % loss

*(K: 1000 / D: Day / W: Week / IR: Indian River / N: Normal value / HP: Hydropericardium /AS: Ascites / RT-PCR: Real Time Polymerase Chain Reaction)

TABLE 2.Results of real time qPCR(ct values) and conventional PCR of the examined samples.

Sample ID	Ct value	Results of conventional PCR (800bp)
1	30	-ve
2	30	-ve
3	32	-ve
4	18	+ve
5	36	-ve
6	8	+ve
7	36	-ve
8	32	-ve
9	14	+ve
10	25	-ve

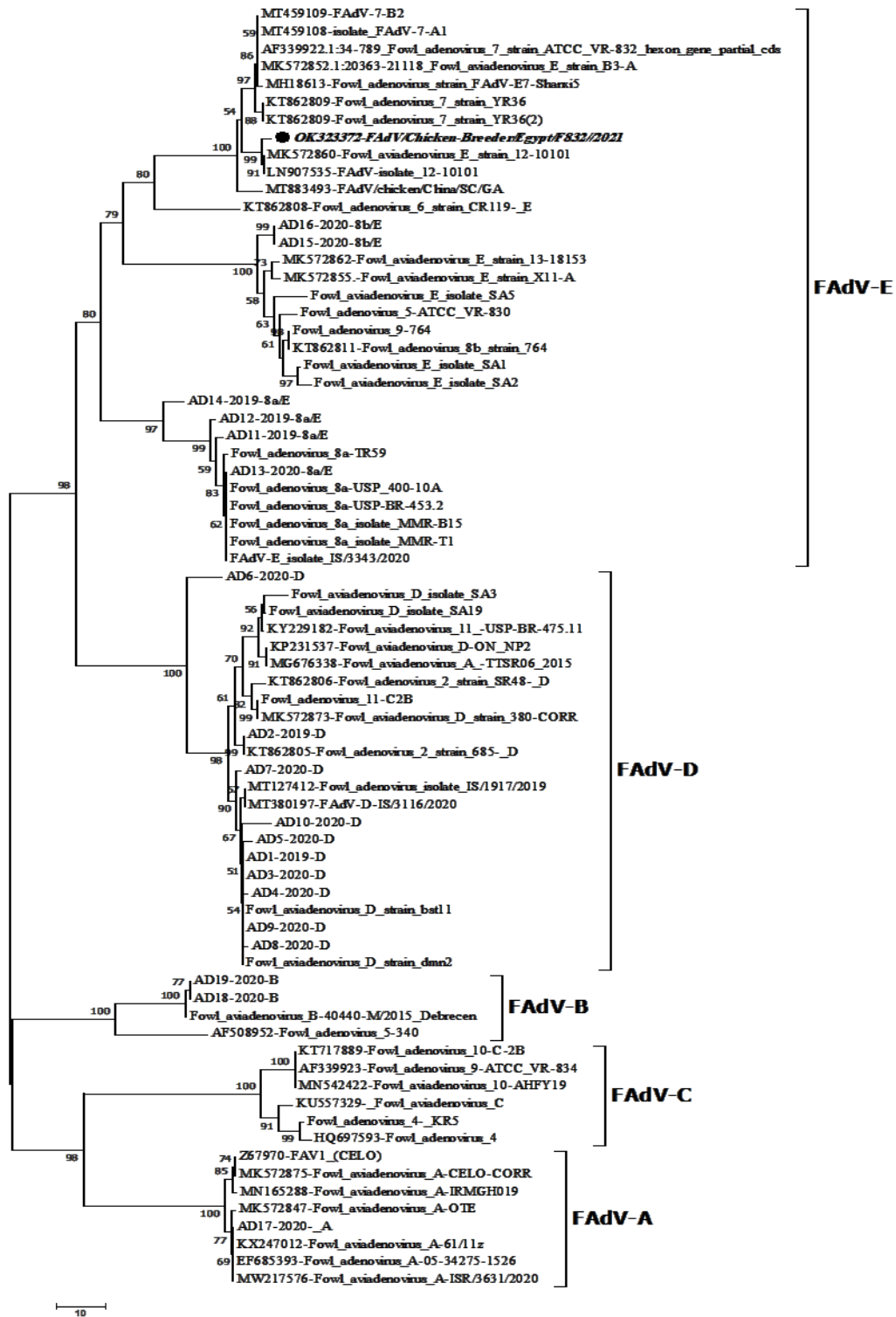


Fig.1. Phylogenetic tree of partial nucleotide sequence of hexon gene; the analysis has been applied on different Fowl adenovirus species. The target sequence of this study is F832-2021 which is labelled with black dot on the tree. F832-2021 belongs genetically to serotype 7 of FAdV-E viruses.

Seq-ID	Nucleotide identity%											
	1	2	3	4	5	6	7	8	9	10	11	12
1 OK323372-Egypt/F832/2021		98.7%	95.7%	94.5%	93.7%	94.7%	83.5%	78.0%	64.9%	53.3%	58.5%	62.6%
2 LN907535-FAdV-isolate 12-10101	97.5%		96.1%	94.9%	94.1%	95.1%	84.3%	78.8%	65.5%	53.7%	58.5%	62.6%
3 MT883493-FAdV/chicken/China/SC/GA	93.3%	95.1%		93.9%	93.1%	94.1%	83.5%	79.6%	65.5%	54.1%	59.1%	62.2%
4 FAdV-7 strain ATCC VR-832	92.7%	94.5%	93.9%		97.7%	99.3%	85.3%	79.6%	66.1%	54.7%	59.5%	62.8%
5 KT862809-FAdV 7 strain YR36	90.9%	92.7%	92.1%	96.3%		98.3%	85.1%	79.4%	65.7%	54.9%	58.7%	63.0%
6 MT459109-FAdV-7-B2	92.1%	93.9%	93.3%	99.3%	96.9%		85.5%	79.8%	66.1%	54.7%	59.3%	62.8%
7 AD16-2020-8b/E	86.0%	87.8%	87.8%	89.0%	87.8%	89.0%		79.0%	65.7%	51.1%	56.1%	60.8%
8 FAdV-8a isolate MMR-T1	80.6%	82.4%	84.2%	82.4%	81.8%	82.4%	81.8%		68.2%	54.5%	56.9%	63.2%
9 AD1-2019-D	70.9%	72.7%	73.9%	73.9%	72.1%	73.9%	71.5%	75.7%		51.1%	55.1%	61.0%
10 KU557329- FAdV-C	47.9%	47.9%	49.1%	47.9%	46.9%	47.3%	44.9%	49.1%	45.7%		60.4%	52.7%
11 AD17-2020- A	53.3%	54.5%	55.1%	53.9%	52.7%	53.3%	52.7%	52.1%	49.0%	58.1%		58.4%
12 AD19-2020-B	61.3%	63.0%	61.9%	63.0%	63.6%	63.0%	61.9%	61.9%	60.7%	45.8%	52.3%	

Amino acid identity%

Fig.2. Identity percent of amino acid and nucleotide sequences of F832-2021 with other Egyptian circulated FAdVs species.

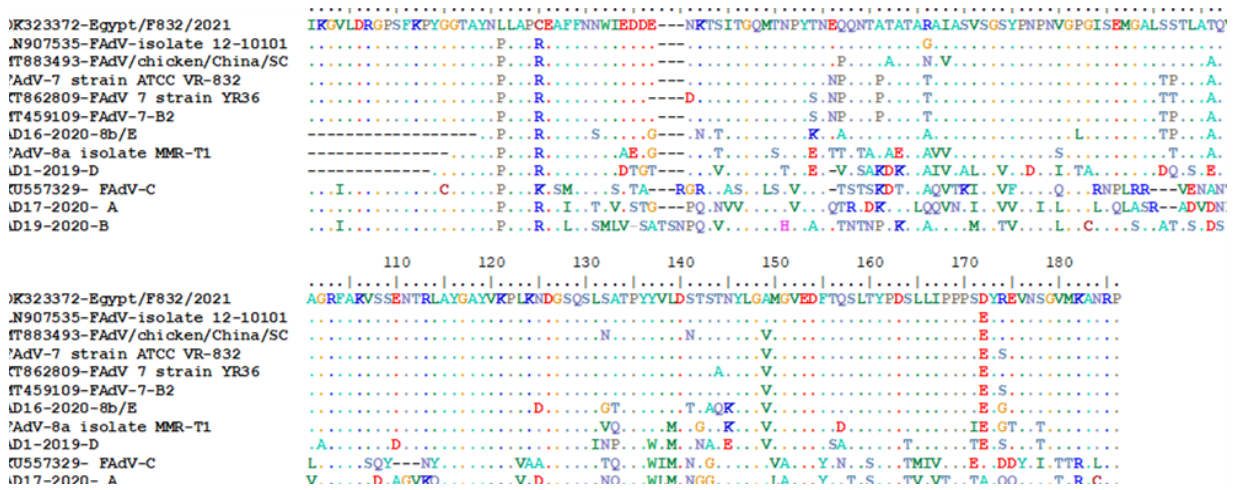


Fig. 3. Amino acid alignment for partial sequences of hexon gene for L1 region of different Egyptian FAdVs.

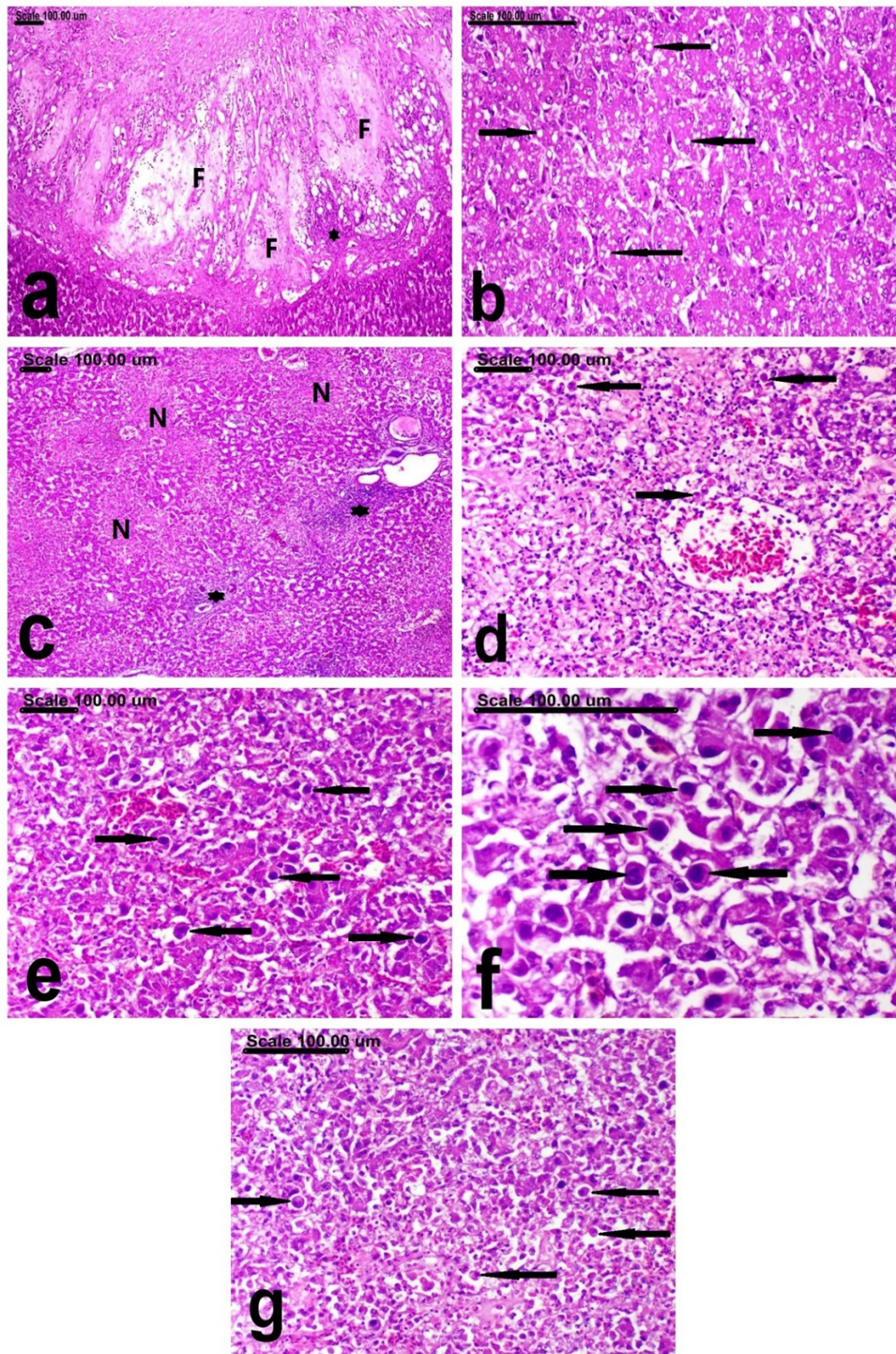


Fig. 4. photomicrograph of the liver of broiler breeders infected with adenovirus showing (a) extensive thickening of the Glisson's capsule with faint pink fibrinous exudates (F) mixed with intense inflammatory cell infiltration, mostly heterophils and lymphocytes (astrix), (b) diffuse vacuolar degeneration of hepatocytes (arrows), (c) bridging hepatocellular necrosis (N) associated with intense leucocytic cellular infiltrates (asterisk), (d) centrilobular necrosis with fragmentation and dissociation of the necrotic hepatocytes in addition to numerous apoptotic cells (arrows), (e , f) inclusion body hepatitis (arrows) (e) with the presence of numerous large basophilic intranuclear inclusions (arrows) (f), and (g) abundant apoptosis (arrows). (Stain: H&E, scale bar=100µm).

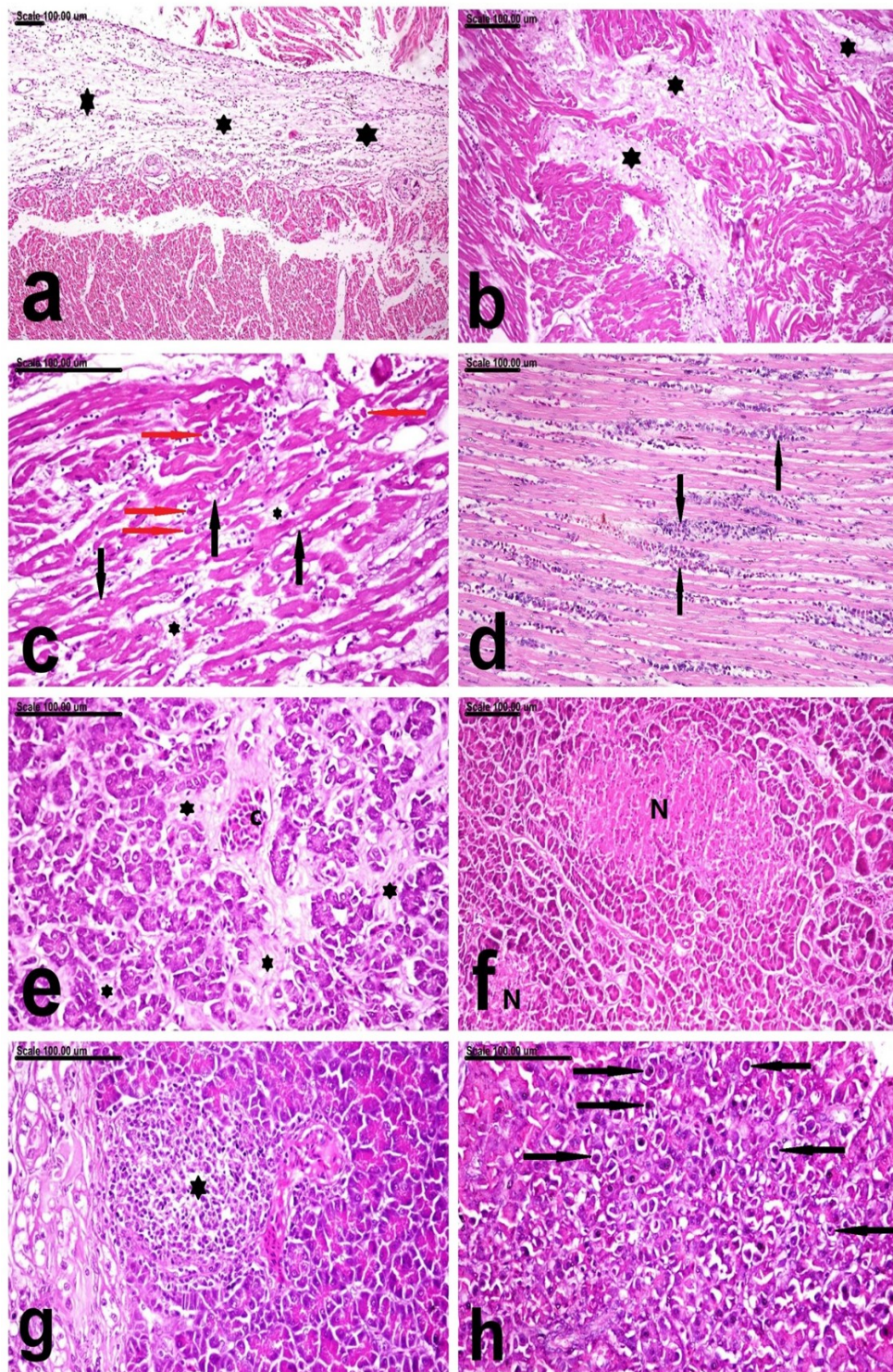


Fig. 5. photomicrograph of the heart (a, b, c, d) and pancreas (e, f, g, h) of broiler breeders infected with adenovirus showing (a) marked thickening of the visceral epicardium by edematous fluid (asterisk) associated with scattered lymphocytic cell infiltration, (b) interstitial edema (asterisk), (c) vacuolar degeneration of cardiomyocytes (black arrows) associated with interstitial edema (asterisk) and numerous apoptoses (red arrows), (d) Interstitial myocarditis with intense infiltration of cardiomyocytes with heterophiles and lymphocyte (arrows), (e, f, g, h) pancreas showing congestion of blood vessels (C) associated with interstitial edema (asterisk) and disruption of pancreatic acinar cells, (f) multifocal areas of pancreatic necrosis with complete loss of cellular architecture that appeared intensely eosinophilic with nuclear pyknosis (N), (g) focal pancreatic necrosis intensely infiltrated with macrophages and lymphocytes (asterisk), and (h) abundant apoptosis of pancreatic acinar cells (arrows). (Stain: H&E, scale bar=100μm).

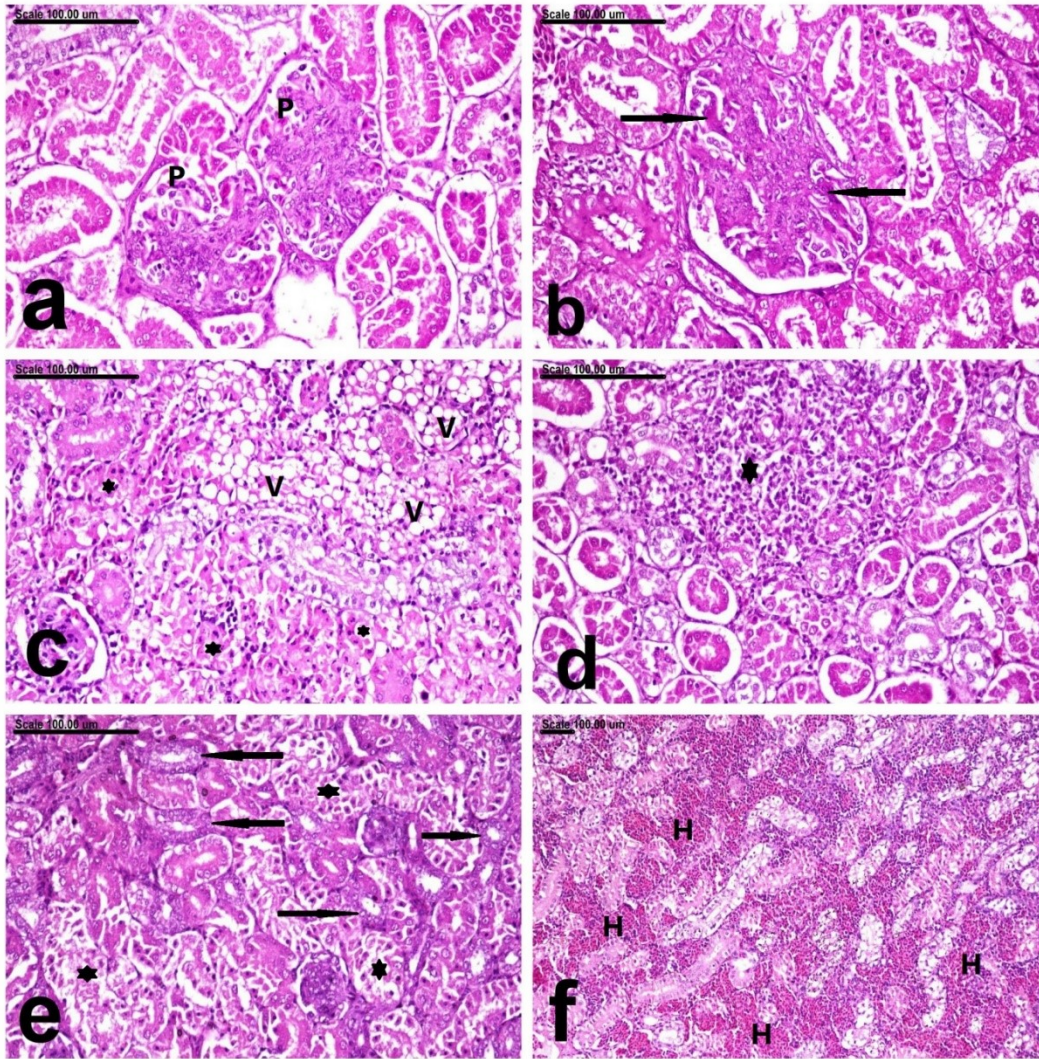


Fig. 6. photomicrograph of the kidneys of broiler breeders infected with adenovirus showing (a) Proliferative glomerulonephritis with markedly swollen glomeruli (p) and obliteration of the Bowman's spaces, (b) membranoproliferative glomerulonephritis, with pronounced mesangial expansion and thickening of glomerular basement membrane (arrows), (c) extensive vacuolar degeneration (V) and extensive necrosis of the renal tubular epithelium (asterisk), (d) intense infiltration of the necrotic renal tubules with inflammatory cells(asterisk), (e) necrotic renal tubules(asterisk) alternate with the regenerative renal tubules, which are lined by large, basophilic vesicular nuclei (arrows), (f) massive interstitial hemorrhage (H), (Stain: H&E, scale bar=100µm).

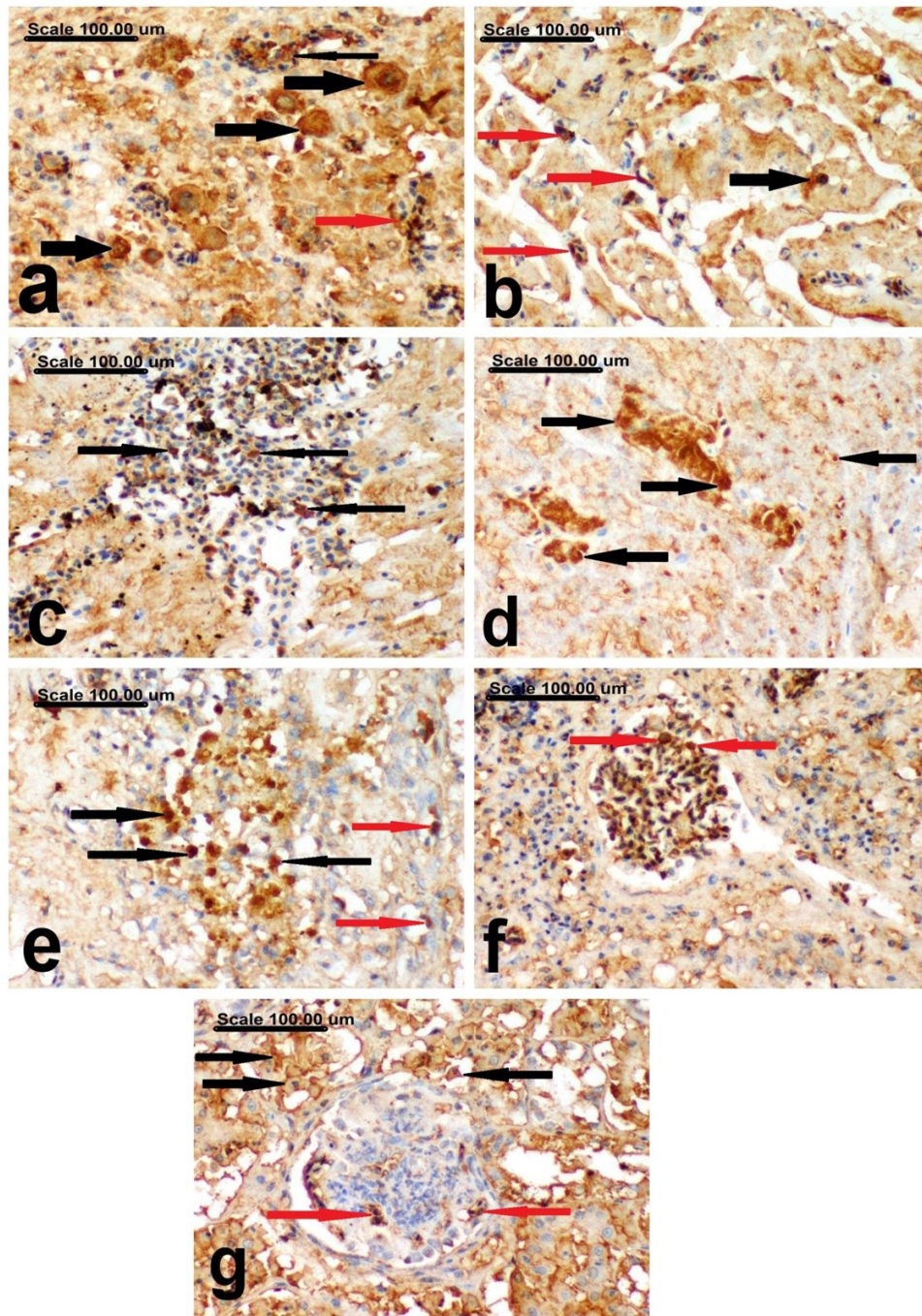


Fig. 7. photomicrograph represent the immunohistochemical detection of adenovirus antigen in the liver, heart, pancreas and kidneys broiler breeders infected with adenovirus: (a) liver showing extensive intranuclear and cytoplasmic staining in the infected hepatocytes (black thick arrows), vascular endothelial cells (black thin arrow), and intravascular leukocytes (red arrow), (b & c) heart showing intense brown intranuclear staining in the cardiomyocytes (black thick arrow), endothelial cells (red arrows) (b) and infiltrating inflammatory leukocytes (black arrows)(c), (d & e) pancreas showing a strong brown intranuclear adenoviral antigen in the pancreatic acinar cells (black arrows)(d), vascular endothelial cells (red arrows) and the infiltrating leukocytes (black arrows) (e), (f & g) kidneys showing brown intranuclear and cytoplasmic adenoviral antigen in the glomerular capillary endothelium (red arrows) (f , g) and renal tubular epithelium (black arrows) (g) (Stain: anti-adenovirus immunohistochemical staining, scale bar=100µm).

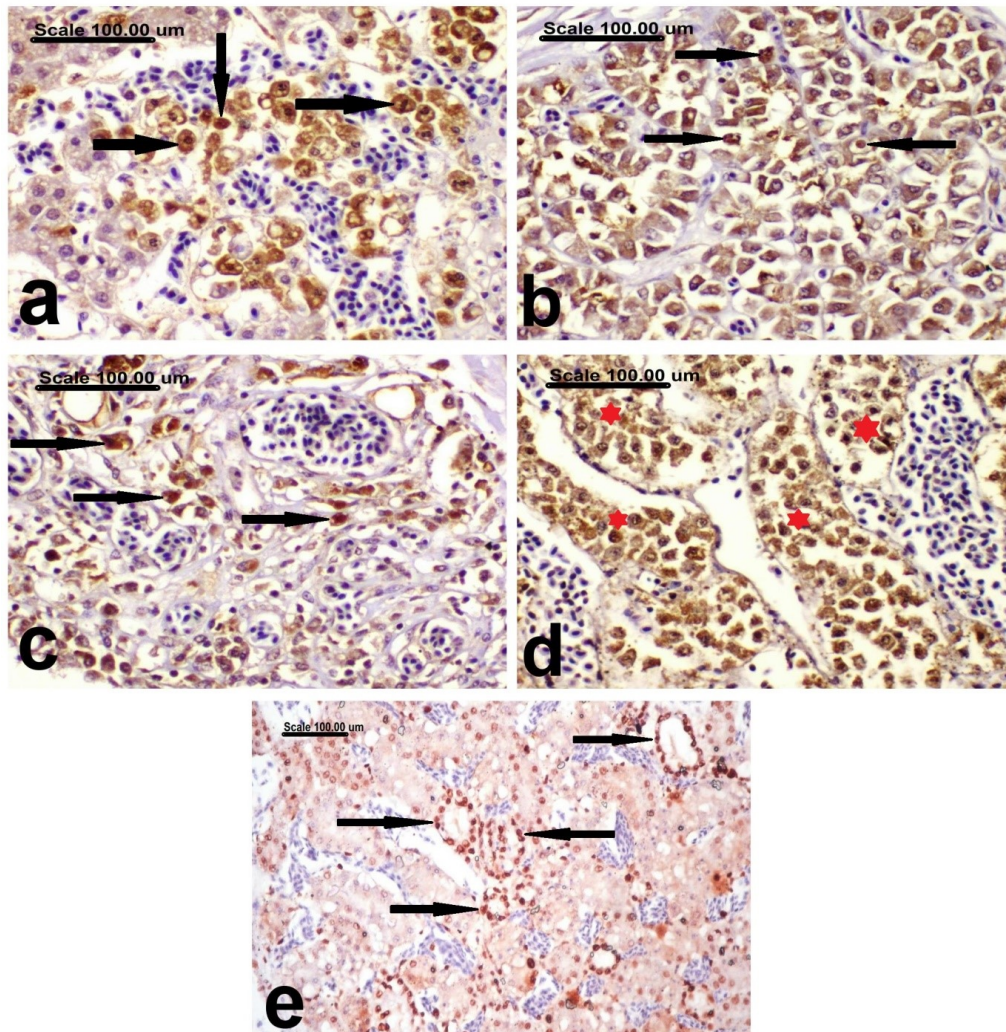


Fig. 8. photomicrograph represent expression of cleaved caspase-3 (a-d) and PCNA (e): (a) liver showing increased caspase-3 expression, with strong brown nuclear and cytoplasmic staining in the hepatocytes (black arrows) (a), (b & c) pancreas showing strong brown nuclear and cytoplasmic staining in the pancreatic acinar cells (black arrows) (b) and the infiltrating macrophages in the area of acute pancreatitis (black arrows) (c), (d) kidneys showing abundant caspase-3-positive cells in the lumen of renal tubules (asterisk), and (e) kidneys showing PCNA-positive cells with strong brown nuclear staining in the regenerating renal tubules (black arrows). (Stain: cleaved caspase-3 (a-d) and PCNA immunohistochemical staining, scale bar=100μm).

References

- McFerran, J.B. and Smyth, J.A.. Avian adenoviruses. *Revue Scientifique et Technique (International Office of Epizootics)*, **19** (2), 589-601 (2000). <https://doi.org/10.1099/0022-1317-81-11-2573>
- Russell, W. Update on adenovirus and its vectors. *Journal of General Virology*, **81**(11), 2573-2604 (2000). <https://doi.org/10.1099/0022-1317-81-11-2573>
- Berk, A.J. Adenoviridae: the viruses and their replication. In Knipe D.M. et al. (ed), *Fields virology*, 5th ed., vol 2. Lippincott Williams & Wilkins, Philadelphia, PA., Pp: 2355–2394 (2007).
- Fitzgerald, S.D.; Rautenschlein, S.; Mahsoub, H.M.; Pierson, F.W.; Reed, W.M. and Jack, S.W. Adenovirus infections. Swayne, D.E., M. Boulianne, C.M. Logue, L.R. McDougald, V. Nair, D.L. Suarez (Eds.), *Diseases of Poultry*, John Wiley & Sons, Inc, Hoboken, NJ, USA, Pp: 321-363(2020). [doi:10.1002/9781119371199.ch9](https://doi.org/10.1002/9781119371199.ch9)
- Smyth, J. A. and McNulty, M. S. (2008). Adenoviridae. In: *Poultry Diseases*. 6th Ed, Pattison, M.; McMullin, P.F.; Bradbury, J. M. and Alexander, D. (eds), Butterworth Heinemann-Elsevier, Pp: 367-381.
- Mase, M.; Mitake, H.; Inoue, T. and Imada, T. Identification of group I-III avian adenovirus by PCR coupled with direct sequencing of the hexon gene. *The Journal of Veterinary Medical Science*, **71**,1239–1242 (2009). <https://doi.org/10.1292/jvms.71.1239>

7. Schachner, A.; Matos, M.; Grafl, B. and Hess, M. Fowl aviadenovirus (FAdV).induced diseases and strategies for their control—a review on the current global situation. *Avian Pathol.*, **47**, 111–126 (2018). <https://doi.org/10.1080/03079457.2017.1385724>
8. Adair, B.M. and Fitzgerald, S.D. (2008). Adenovirus infections. In: Saif, Y.M. Diseases of Poultry. 12th Ed., Ames, Iowa: Iowa State, Pp: 251-296.
9. Yıldırım, Z. and Yalçınalp, M. Preparing Broiler Breeder Females for Optimum Production. *International Poultry Science Congress of WPSA Turkish Branch*, 56 –61(2018).
10. El-Tholoth, M. and Abou El-Azm, K.I. Molecular detection and characterization of fowl adenovirus associated with inclusion body hepatitis from broiler chickens in Egypt. *Tropical Animal Health and Production*, **51**,1065–1071 (2019). doi: 10.1007/s11250-018-01783-0
11. El-Basrey, Y. F.; Hamed, R. I.; Mohamed, M. and LebDAH, M. A. Detection of Inclusion Body Hepatitis Virus in broilers at Sharkia Province, Egypt. *Journal Animal Health Production*, **9**(s1), 84-89(2020). [.10.3382/ps/pey314](https://doi.org/10.3382/ps/pey314): <http://dx.doi.org/10.17582/journal.jahp/2020/9.s1.84.89>
12. Elbestawy, A.R.; Ibrahim, M.; Hammam, H.; Noreldin, A.E.; Bahrawyand El, Ellakany, H.F. Molecular Characterization of Fowl Adenovirus D Species in Broiler Chickens with Inclusion Body Hepatitis in Egypt. *Alexandria Journal of Veterinary Sciences*, **64** (1),110-117(2020). doi: 10.5455/ajvs.74411
13. Adel, A.; Mohamed, A.A.E.; Samir, M.; Hagag, N.M.; Erfan, A.; Said, M.; Hassan, W.M.M.; El Zowalaty, M.E. and Shahien, M.A. Epidemiological and molecular analysis of circulating fowl adenoviruses and emerging of serotypes 1, 3, and 8b in Egypt. *Heliyon*, **7**, e08366, 1-11(2021). doi: 10.1016/j.heliyon.2021.e08366
14. Radwan, M.M.; El-Deeb, A.H.; Mousa, M.R.; El-Sanousi, A.A. and Shalaby, M.A. First report of fowl adenovirus 8a from commercial broiler chickens in Egypt: molecular characterization and pathogenicity. *Poultry Science*, **98**, 97–104(2019). doi: 10.3382/ps/pey314
15. Sultan, H.; Arafa, A.E.S.; Adel, A.; Selim, K.; El-Hoseni; M. and Talaat, S. Genetic characterization of Novel fowl aviadenovirus-4 (FADV-4) from the outbreak of hepatitis-hydropericardium syndrome in commercial broiler chickens in EgyptNovel FAdV-4 in Egypt. *Avian Disease*, 21-23(2021). doi: 10.1637/0005-2086-65.3.385
16. Hall, T.A. BioEdit: a user-friendly biological sequence alignment editor and analysis program for Windows 95/98/NT, in: Nucleic Acids Symposium Series. [London]: Information Retrieval Ltd., c1979-c2000., Pp. 95–98(1999)..
17. Kumar, S.; Stecher, G.; Li, M.; Knyaz, C. and Tamura, K. MEGAX. molecular evolutionary genetics analysis across computing platforms. *Molecular Biology and Evolution*, **35**(6),1547-1549 (2018). .doi: 10.1093/molbev/msy096
18. Kim, S.; Layon, C. and Bancroft, J. (2013): Bancroft Theory and Practice of histological techniques. Churchill Livingtone. Elsevier Health Sciences, 7th edition.
19. Wilson, F.D.; Wills, R.W.; Senties-Cue, C.G.; Maslin, W.R.; Stayer, P.A. and Magee, D.L. High incidence of glomerulonephritis associated with inclusion body hepatitis in broiler chickens: Routine histopathology and histomorphometric studies. *Avian Dis.*, **54**, 975–980(2010). doi: 10.1637/9050-090709-Reg.1
20. Leenaars, M. and Hendriksen, C.F.M. Critical steps in the production of polyclonal and monoclonal antibodies: evaluation and recommendations. *ILAR Journal*, **46**(3), 269-279(2005). doi: 10.1093/ilar.46.3.269
21. Schunk, M.K. and Macallum, G.E. Applications and Optimization of Immune Procedures. *ILAR Journal*, **46**(3), 241-257(2005). doi: 10.1093/ilar.46.3.241
22. Gesek, M., Paździor, K., Otrocka-Domagala, I., Rotkiewicz, T. and Szarek, J. Fibromuscular dysplasia in arteries and in a vein in broiler chickens. *Pol. J. Vet. Sci.*, **16**(1),93-99(2013). PMID: 23691581;doi: 10.2478/pjvs-2013-0013
23. Killian, M.P., Boviez, J.D., Gambarotta, M., Lombardo, D.M. Induction of apoptosis in the bursa of Fabricius by vaccination against Gumboro disease. *Avian Pathol.*, **46**(5), 526-534(2017). Epub 2017 Jun 19. PMID: 28447468doi: 10.1080/03079457.2017.1322684
24. Günes, A.; Marek, A.; Grafl, B.; Berger, E. and Hess, M. Real-time PCR assay for universal detection and quantitation of all five species of fowl adenoviruses (FAdV-A to FAdV-E). *Journal of Virological Methods*, **183**, 147–153 (2012). .doi: 10.1016/j.jviromet.2012.04.005
25. Savage, C.J.; Middleton, D. and Studdert, M.J. (2013). Adeno, hendra, and equine rhinitis viral respiratory diseases. *Equine Infection Disease* . 2nd (Ed.); Sellon, DC, Long, MT, Pp:189–197.doi:10.1016/B978-1-4557-0891-8.00017-8
26. Niczyporuk, J.S. Deep analysis of Loop L1 HVRs1-4 region of the hexon gene of adenovirus field strains isolated in Poland. *PLoS One*, **13**, e0207668 (2018). <https://doi.org/10.1371/journal.pone.0207668>
27. Schachner, A.; Gonzalez; G., Endler; L., Ito, K. and Hess, M. Fowl adenovirus (FAdV) recombination with intertypic crossovers in genomes of FAdV-D and FAdV-E, displaying hybrid serological phenotypes. *Viruses*, **11**, 1094, 1-23(2019). doi: 10.3390/v11121094
28. Mittal, D.; Jindal, N.; Tiwari, A.K. and Khokhar, R.S. Characterization of fowl adenoviruses associated with hydropericardium syndrome and inclusion body hepatitis in broiler chickens. *Virus Disease*, **25**(1),114-119(2014). doi: 10.1007/s13337-013-0183-7

29. Changjing, L.; Haiying, L.; Dongdong, W.; Jingjing, W.; Youming, W.; Shouchun W.; Jida, L.; Ping, L.; Jianlin, W.; Shouzhen, X.; Shangjin, C.; Yi, Z. and Yanbo, Y. Characterization of fowl adenoviruses isolated between 2007 and 2014 in China. *Vet. Microbiol.*, **197**, 62-67(2016). doi: 10.14202/vetworld.2020.981-986
30. Liu, J.; Shi, X.; Lv, L.; Wang, K.; Yang, Z.; Li, Y. and Chen, H. Characterization of Co-infection With Fowl Adenovirus Serotype 4 and 8a. *Front. Microbiol.*, **12**, 771805(2021). doi: 10.3389/fmicb.2021.771805
31. Hosseini, H.; Najafi, H.; FallahMehrabadi M.H.; Gholamian, B.; Noroozi, S.; Ahmadi, M.; Ziafati, K.Z.; Sadri, N.; HojabrRajeoni, A. and Ghalyanchilangeroudi, A. Molecular detection of fowl adenovirus 7 from slaughtered broiler chickens in Iran: the first report. *Iran J. Vet. Res.*, **22**(3), 244-247 (2021). doi: 10.22099/ijvr.2021.37426.5452
32. Mirzazadeh, A.; Asasi, K.; Schachner, A.; Mosleh, N.; Liebhart, D.; Hess, M. and Grafl, B. Gizzard Erosion Associated with Fowl Adenovirus Infection in Slaughtered Broiler Chickens in Iran. *Avian Dis.*, **63**(4), 568-576(2019).. doi: 10.1637/aviandiseases-D-19-00069
33. Schachner, A.; Grafl, B. and Hess, M. Spotlight on avian pathology: fowl adenovirus (FAdV) in chickens and beyond – an unresolved host-pathogen interplay. *Avian Pathology*, **50**, 1, 2-5(2021). doi: 10.1080/03079457.2020.1810629
34. Niczyporuk, J.S.; Kozdrun, W.; Czekaj, H. and Piekarska, K. Characterisation of adenovirus strains represented species B and E isolated from broiler chicken in eastern Poland. *Heliyon*, **7** (2), e06225 (2021). doi: 10.1016/j.heliyon.2021.e06225
35. Khodakaram-Tafti, A., Asasi, K. & Namazi, F. Clinicopathological characteristics of acute inclusion body hepatitis outbreak in broiler chickens in Iran. *Bulg. J. Vet. Med.*, **19**(2), 163–116(2016). doi: 10.15547/bjvm.926
36. Schachner, A.; Marek, A.; Jaskulska, B.; Bilic, I. and Hess, M. Recombinant FAdV-4 fiber-2 protein protects chickens against hepatitis-hydropericardium syndrome (HHS). *Vaccine*, **32**, 1086–1092(2014). doi: 10.1016/j.vaccine.2013.12.056
37. Ilyas, G.; Zhao, E.; Liu, K.; Lin, Y.; Tesfa, L.; Tanaka, K.E. and Czaja, M.J. Macrophage autophagy limits acute toxic liver injury in mice through down regulation of interleukin-1. *J. Hepatol.*, **64**, 118–127 (2016). doi: 10.1016/j.jhep.2015.08.019
38. Niu, Y.; Sun, Q.; Zhang, G.; Liu, X.; Shang, Y.; Xiao, Y. and Liu, S. Fowl adenovirus serotype 4-induced apoptosis, autophagy, and a severe inflammatory response in liver. *Vet. Microbiol.*, **223**, 34–41(2018). doi: 10.1016/j.vetmic.2018.07.014
39. Zhao, M.; Duan, X.; Wang, Y.; Gao, L.; Cao, H.; Li, X. and Zheng, S.J. A novel role for px, a structural protein of fowl adenovirus serotype 4 (fadV4), as an apoptosis-inducer in leghorn male hepatocellular cell. *Viruses*, **12**(2), 228(2020). doi: 10.3390/v12020228
40. Haiyilati, A.; Li, X. and Zheng, S. Fowl Adenovirus: Pathogenesis and Control. *International Journal of Plant, Animal and Environmental Sciences*, **11**, 566-589 (2021). doi: 10.26502/ijpaes.202122
41. Tsiouris, V.; Mantzios, T.; Kiskinis, K.; Guérin, J.-L.; Croville, G.; Brellou, G.D.; Apostolopoulou, E.P.; Petridou, E.J. and Georgopoulou, I. First detection and identification of fadv-8b as the causative agent of an outbreak of inclusion body hepatitis in a commercial broiler farm in Greece. *Vet. Sci.*, **9**, 160(2022). doi: 10.3390/vetsci9040160
42. Lopes, M.C.; FreitasNeto, O.C.; Amaral, C.I.; Lacerda, M.S.C.; Fonseca, C.S.; Martins, N.R.S. and Ecco, R. Hepatic changes in Gallus gallus domesticus in Brazil. *Pesquisa Veterinária Brasileira*, **42**, e07078(2022). doi:10.1590/1678-5150-pvb-7078
43. Mughal, S.A.; Ahmed, G.; Hussain, T.; Fazlani, S.A.; Ahmed, I. and Khan, F.A. In vivo pathogenicity of hydropericardium hepatitis syndrome (Angara disease). *African Journal of Biotechnology*, **10**, 13664-13671(2011). doi:10.5897/AJB10.2506
44. Kumar, V.; Kumar, R.; Chandra, R.; Bhatt, P. and Dhama, K. Outbreaks of inclusion body hepatitis (IBH) in chickens; pathological studies and isolation of fowl adenovirus. *Adv. Anim. Vet. Sci.*, **1** (3S), 21 – 24 (2013). <http://www.nexusacademicpublishers.com/journal/4>
45. Chen, Z.; Shi, S.; Qi, B.; Lin, S.; Chen, C.; Zhu, C. and Huang, Y. Hydropericardium syndrome caused by fowl adenovirus serotype 4 in replacement pullets. *J. Vet. Med. Sci.*, **81**(2), 245-251(2019). doi: 10.1292/jvms.18-0168
46. Niu, Y.; Sun, Q.; Liu, X. and Liu, S. Mechanism of fowl adenovirus serotype 4-induced heart damage and formation of pericardial effusion. *Poultry Science*, **98** (3), 1134-1145(2019). doi: 10.3382/ps/pey485
47. Miguel M., Beatrice G., Dieter L., Ilse S. and Michael H. Selected clinical chemistry analytes correlate with the pathogenesis of inclusion body hepatitis experimentally induced by fowl aviadenoviruses. *Avian Pathology*, **45**(5), 520-529 (2016). doi: 10.1080/03079457.2016.1168513
48. Rahimi, M. and Minoosh, S.H.Z. Adenovirus-like inclusion body hepatitis in a flock of broiler chickens in Kermanshah province, Iran. *Vet. Res. Forum*, **6**(1), 95-98(2015).. <https://www.ncbi.nlm.nih.gov/pmc/articles/PMC4405693/>
49. Panigrahi, S.; Swain, K.; Routray, A.; PrakashRath, A.; Sahoo, S. and Ganguly, S. Inclusion body hepatitis and hydropericardium syndrome in poultry: A Brief Review. *ARC Journal of Animal and Veterinary Sciences (AJAVS)*, **2** (4), 12-14(2016). ISSN 2455-2518. doi:10.20431/2455-2518.0204002

50. Piek, A.; de Boer, R. A. and Sillje, H. H. The fibrosis-cell death axis in heart failure. *Heart Fail. Rev.*, **21**, 199–211(2016). doi: 10.1007/s10741-016-9536-9
51. Puhlmann, M. ;Weinreich, D.M.; Farma, J.M.; Carroll, N.M.; Turner, E.M. and Alexander, H.R. Interleukin-1beta induced vascular permeability is dependent on induction of endothelial tissue factor (TF) activity. *J. Transl. Med.*, **3**, 37(2005). doi: 10.1186/1479-5876-3-37
52. Fitzgerald, S.D. and Adair, B.M. (2008). Group 1 adenovirus infections. In: Diseases of poultry, 12th ed. Y.M. Saif, ed. Blackwell Publishing ,Ames , IA, pp.252-266.
https://doi.org/10.1002/9781119371199.ch9
53. Wisma Tani, P. Avian adenovirus isolated from broiler affected with inclusion body hepatitis. *Malaysian Journal of Veterinary Research*, **7** (2), 121-126 (2016).
https://www.dvs.gov.my/dvs/resources/user_14/MJV R_V7N2/MJVR-V7N2-p121-126.pdf
54. Mariappan, A.K.; Munusamy, P.; Latheef, S.K.; Singh, S.D. and Dhama, K. HepatoNephropathology associated with Inclusion Body Hepatitis complicated with citrininmycotoxicosis in a broiler farm. *Veterinary World*, **11**(2), 112-117(2018). doi: 10.14202/vetworld.2018.112-117
55. Schmidt, R.E. Types of renal disease in avian species. *Vet. Clin. North Am. Exot. Anim. Pract.*, **9**(1), 97-106(2006). doi: 10.1016/j.cvex.2005.10.003
56. De Herdt, P.; Timmerman, T.; Defoort, P.; Lycke, K. and Jaspers, R. Fowl adenovirus infections in Belgian broilers: a ten-year survey. *Vlaams Diergeneeskundig Tijdschrift* **82**(3), 125-133 (2013). doi: https://doi.org/10.21825/vdt.v82i3.16704
57. Matos, M.; Grafl, B.; Liebhart, D. and Hess, M. The outcome of experimentally induced inclusion body hepatitis (IBH) by fowl aviadenoviruses (FAdVs) is crucially influenced by the genetic background of the host. *Veterinary Research*, **47**, 69(2016). doi: 10.1186/s13567-016-0350-0
58. Wang, K.; Sun, H.; Li, Y.; Yang, Z.; Ye, J. and Chen, H. Characterization and pathogenicity of fowl adenovirus serotype 4 isolated from eastern China. *BMC Vet. Res.*, **15**(1), 373(2019). doi: 10.1186/s12917-019-2092-5
59. Chen, L., Yin, L., Peng, P., Zhou, Q., Du, Y., Zhang, Y., Xue, C. and Cao, Y. Isolation and Characterization of A Novel Fowl Adenovirus Serotype 8a Strain from China. *Viol. Sin.*, **35**(5), 517-527 (2020). doi: 10.1007/s12250-019-00172-7
60. Alcigir, M.E. and Atalay, V. Evaluation of liver and heart lesions induced by experimental fowl adenovirus-4 infection in broilers and virus detection by immunohistochemistry, immunofluorescence and in situ PCR. *Revue Méd. Vét.*, **164**(7), 348–57(2013).
https://www.researchgate.net/publication/289664356
61. Niu, Y.; Sun, Q.; Zhu, M.; Zhao, J.; Zhang, G.; Liu, X.; Xiao, Y. and Liu S. Molecular epidemiology and phylogenetic analysis of fowl adenoviruses caused hydropericardium outbreak in China during 2015. *Poult Sci.*, **97**(3), 803-811(2018).
https://doi.org/10.3382/ps/pex338
62. Rodrigues, R.B.; Motta, R.R.; Machado, S.S.; Cambuzzi, E.; Zettler, E.W.; Zettler, C.G. and Jotz, G.P. Prognostic value of the immunohistochemistry correlation of Ki-67 and p53 in squamous cell carcinomas of the larynx. *Brazilian Journal of Otorhinolaryngology*, **74** (6), 855-859(2008). doi: 10.1016/S1808-8694(15)30145-2
63. Su, J. and Zheng, J. Use of tumor proliferation marker ki-67 and PCNA in surgical pathology. *Zhonghuabing li xuezhazhi Chinese Journal of Pathology*, **38**(8), 568-571 (2009).
https://doi.org/10.3760/CMA.J.ISSN.0529-5807.2009.08.0 21
64. Banlunara, W.; Bintvihok, A. and Kumagai, S. Immunohistochemical study of proliferating cell nuclear antigen (PCNA) in duckling liver fed with aflatoxin B1 and esterified glucomannan. *Toxicon*, **46**,954-957(2005). doi: 10.1016/j.toxicon.2005.04.019

الخصائص الجزيئية والنسجية المرضية والكيميائية المناعية عن اول تسجيل لفيروس غدى الدواجن النمط المصلى 7 من النوع E فى امهات الدجاج اللاحم فى مصر.

محمد حلمى¹، امانى عادل²، عزه حسن³ و روجيه دغيم³

¹ الشركة القابضة للمستحضرات الحيوية واللقاحات (فاكسيرا)- الدقى-الجيزة- مصر

² المعمل المرجعى للرقابه البيطرية على الانتاج الداجنى- الدقى- الجيزة- مصر

³ قسم الباثولوجيا-كلية الطب البيطرى-جامعة القاهرة- الجيزة -مصر

الملخص

أصبحت الفيروسات الغدية للدواجن مؤخرًا موضوعًا ساخنًا لغالبية الباحثين والمحققين المصريين حيث عانت صناعة الدواجن المصرية من عدة حالات تفشى لهجمات الفيروسات الغديه فى قطعان الدجاج اللاحم التجارى. نظرًا لان الانتقال الراسى من قطيع الامهات يمثل الطريق الاكثر شيوعا للعدوى، فقد هدفت الدراسة الحاليه الى دراسة الفيروس الغدى المعزول من قطعان امهات الدجاج اللاحم التجارية فى شمال مصر خلال الفترة من 2021 إلى 2023. بعد ظهور حالات النفوق المفاجى وانخفاض انتاجية البيض. الصفات التشريحية الملاحظه كانت تغير لون الكبد مع مظهر مزرقش، وارتشاح التامور فى القلب وشكل غير طبيعى للكلى.

تم فحص عينات الاعضاء والمسحات من 10 قطعان الامهات بتفاعل البوليميراز المتسلسل. كشف تحليل تفاعل البوليميراز عن ايجابية الفيروس الغدى للدواجن مع قيم عتبة الدورة ((CT متغيرة تتراوح من 10 الى 36. تم تضخيم الحلقة 1 (مناطق L 1) على الجين السداسى للعينات الايجابية العشر بواسطة تفاعل البوليميراز المتسلسل التقليدى مما نتج عنه ايجابية ثلاث عينات فقط ذات حجم الجزيئى 800 زوج قاعدى. تم عمل تسلسل الحمض النووى لمنطقة L 1 لعينه واحدة تمثليه. كشف التوصيف الوراثى عن اول تسجيل لوجود النمط المصلى 7 من النوع FAV-E فى مصر. العينه المتسلسلة تشبه السلالة 10101-12 بتماثل 97%. وقد ظهر الالتهاب الكبدى الاشمالى وموت الخلايا المبرمج الغزير فى الكبد والبنكرياس والكلى فى المقاطع النسيجه. علاوة على ذلك تم اظهار مستضد FAV فى الانسجة المختلفة باستخدام بيروكسيداز-أفيدين-بيوتين. بالاضافه الى ذلك هناك تلوخ مناعى قوى ايجابى ل Caspase-3 وPCNA. كشف الفحص النسيجى المرضى عن وجود الالتهاب الكبدى الاشمالى المصاحب بموت الخلايا المبرمج الغزير، نخر خلايا البنكرياس والتهاب كبيبات الكلى، والنخر الانبويى الحاد. علاوة على ارتشاح شديد والتهاب فى عضلة القلب وقد تم اظهار مستضد FAV فى الانسجة المختلفة باستخدام بيروكسيداز-أفيدين-بيوتين. بالاضافة الى ذلك، اظهر تلوخ كاسباس 3- المشقوق الكيمائى الهستولوجى المناعى تفاعل مناعى ايجابى قوى فى الكبد والبنكرياس والكليتين. كشف تلوخ PCNA المناعى عن تفاعل مناعى ايجابى فى الانابيب الكلوية المتجددة.

الكلمات الداله: الفيروس الغدى للطيور، الفحص النسيجى المرضى ، كاسباس-3، PCNA ، كيمياء الهستولوجيا المناعية.